DOI: 10.1002/anie.200604718

Biomaterials

The Amphiphilic Properties of Spider Silks Are Important for Spinning**

*Josef H. Exler, Daniel Hümmerich, and Thomas Scheibel**

Over the course of 300 million years, spiders evolved to become outstanding silk producers. In contrast to insects, such as the silkworm *Bombyx mori*, orb-weaving spiders can produce up to seven different silks for different purposes. Of these silks, those produced in major ampullate glands are the most thoroughly investigated. Major ampullate silks (MAS) are employed for building the frame and radii of the orb web as well as the life lines used to escape predators.[1,2] MAS threads are composed of two proteins and display excellent mechanical properties exceeding those of the best manmade fibers; for example, MAS threads are tougher than even Kevlar. Unfortunately, silks cannot be retrieved from spiders (e.g. by farming) for technical applications because of their territorial and cannibalistic behavior. During the last two decades, progress in genetic engineering has made the biotechnological production of spider silk proteins possible.[1] Since spider silk fibers are envisioned for various medical and technical applications, scientists have further focused on developing an artificial silk spinning process.[1,3] In general, the spinning of spider silk corresponds to a transition from a liquid phase to a solid thread. This liquid–solid transition is initiated in the spider's spinning duct by variation of parameters such as pH, ionic strength, and the concentration of lyotropic ions.[4a,5]

We have previously developed a method to biotechnologically produce the genetically engineered silk protein eADF3 (with a purity of $>99\,\%$) mimicking the known sequence of ADF3, one of the two MAS proteins of the garden spider *Araneus diadematus*.[1,6] Here, we report on details of the liquid–solid transition of eADF3 starting from solution.

Based on its amino acid sequence, eADF3 is an amphiphilic protein with a monomeric molecular weight (MW) of 106 kDa (Figure 1).[4c,6] The protein is characterized by a repetitive amino-terminal domain (1073 amino acids) and a carboxy-terminal nonrepetitive (NR) domain (123 amino acids) responsible for dimerization of the protein. The NR domain contains the only cysteine residue in the protein and can form an intermolecular disulfide bridge. Lyophilized eADF3 can be dissolved only in protein denaturants such as guanidinium thiocyanate. Previously, we have shown that

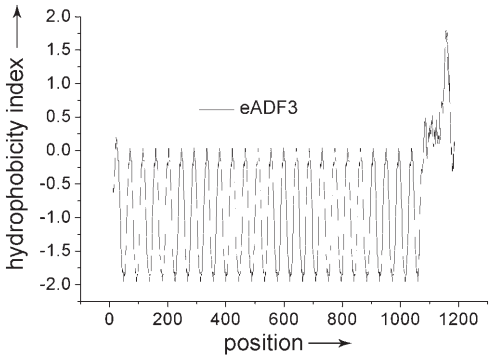

Figure 1. Hydrophobicity plot of eADF3. The repetitive sequence of the amino-terminal domain results in an amphiphilic pattern with altering hydrophilic and hydrophobic patches. The position at the *x* axis reflects the corresponding amino acid of the protein, starting at the amino terminus and ending at the carboxy terminus. The hydrophobicity index relates the relative hydrophobicity among amino acids; more positive values indicates stronger hydrophobicity. In a protein, hydrophobic amino acids are more likely to be located in the interior of its structure, whereas hydrophilic amino acids are more likely to face the aqueous environment.

after dialysis against aqueous buffers eADF-3 displays an intrinsically unfolded secondary structure in the repetitive domain and an α-helical structure in the NR domain (Figure 2).[1,6]

Strikingly, upon dialysis with aqueous buffers a liquid–liquid phase separation of eADF3 is initiated (Figures 3 and 4). One of the two emerging phases has a viscosity of $\eta = 61.8$ mPa s (in comparison, the viscosity of olive oil is $\eta = 100$ mPa s) and protein concentrations higher than 1.4 mM

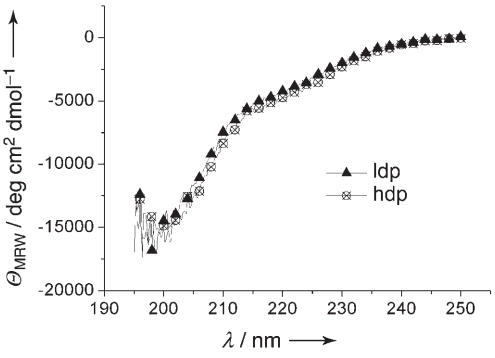

Figure 2. Secondary-structure analysis of eADF3 in solution. Far-UV CD measurements of the low-density and the high-density phases of eADF3 (1.5 μM) in 10 mM Tris/HCl, pH 8, at 20 °C. The spectra are not influenced by sample dilution and are identical under reducing and oxidizing conditions. ldp: low-density phase; hdp: high-density phase.

[*] J. H. Exler, Dr. D. Hümmerich, Dr. T. Scheibel
Department Chemie, Lehrstuhl Biotechnologie
Technische Universität München
Lichtenbergstrasse 4, 85747 Garching (Germany)
Fax: (+49) 89-289-13345
E-mail: thomas.scheibel@ch.tum.de

[**] This work was supported by the Deutsche Forschungsgemeinschaft (SCHE 603/4-1, 4-2).

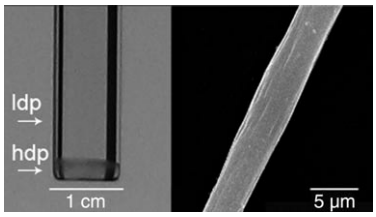

Figure 3. Phase separation of eADF3 upon dialysis. In the left panel, both phases are shown in a 1-mL glass cuvette after dialysis. The high-density phase (hdp) is seen at the bottom and the low-density phase (ldp) on top. In the right panel, a SEM picture depicts a silk thread drawn from the high-density phase.

(Figure 4). This high-density phase contains eADF3 oligomers (MW > 30.000 kDa as determined by dynamic light scattering), which are noncovalently associated. Importantly, upon addition of potassium phosphate, one of the natural triggers of silk assembly, β-sheet-rich threads can be immediately drawn from this phase (Figure 3).

The second phase exhibits concentrations between 150 and 200 μM and a viscosity of $\eta = 1.6$ mPa s, comparable to water with $\eta = 1.0$ mPa s, and consists of solely dimeric protein (MW = 212 kDa). Drawing stable silk threads out of this phase is not possible under the conditions employed. Interestingly, the secondary structure of soluble eADF-3 is identical in both phases (Figure 2). Therefore, it is not a change in secondary structure but in the oligomeric state that is crucial for fiber formation.

High sodium chloride concentrations, as found in the spider's silk glands,[5] completely inhibit oligomer formation as the hydrophilic interactions of the silk protein with the solvent dominate. Additionally, hydrophobic interactions within the silk protein are weakened. As a result, no liquid–liquid phase separation occurs (Figure 4a). In the spider's silk gland only a one-phase solution exists with extremely high protein concentrations of up to 40% w/v. Our finding provides an explanation for why the liquid–solid transition is inhibited in the spider's gland (where it is extremely harmful for the animal). Although the proteins are highly concentrated in the lumen of the gland, we assume that high concentrations of sodium chloride inhibit the formation of the silk oligomers, which are required for thread assembly.[4] As soon as sodium chloride is removed, oligomers assemble in our experiments. In spiders, it has been detected that the high sodium chloride concentrations are decreased when silk proteins pass through the spinning duct, likely also enabling silk oligomerization.

Within the natural spinning process, pH changes are another critical parameter. During the passage of the proteins through the spinning duct, the pH is decreased to 6.3 before threads are spun.[5] Therefore, we tested the pH dependence of phase separation and detected that at pH values above 8.5 liquid–liquid phase separation is also inhibited (Figure 4b), likely because some of the 51 tyrosine residues (usually uncharged) of eADF3 deprotonate above pH 9.[7] The anionic tyrosylates of the hydrophobic blocks increase the hydrophilicity and reduce the hydrophobic interactions. This

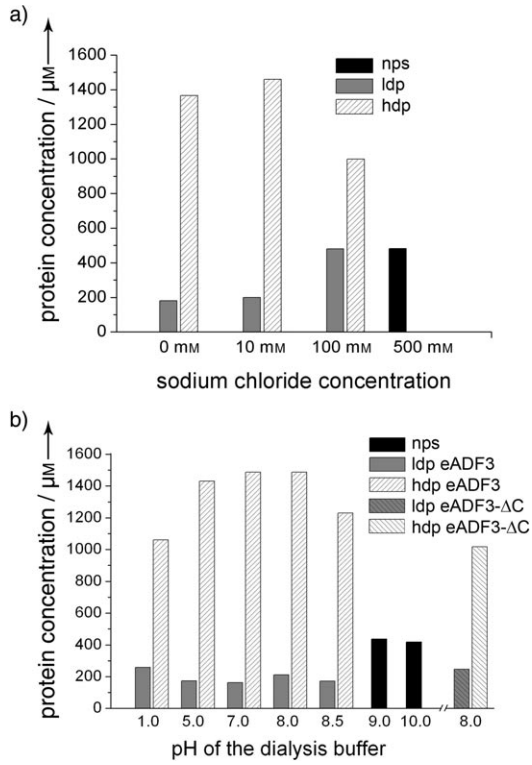

Figure 4. a) Concentrations of the high-density and the low-density phases of eADF3 after addition of sodium chloride to the dialysis buffer. The concentration of the high-density phase (> 15% w/v) is similar to that in silk glands. b) Influence of pH on the phase separation of eADF3 and eADF3-ΔC. nps: no phase separation; ldp: low-density phase; hdp: high-density phase.

phenomenon results in suppression of protein oligomerization. Together with the effect of sodium chloride, adjustment of the pH allows the precise control of silk protein oligomerization and assembly.

Next, we qualitatively compared eADF3 with the NR deletion mutant eADF3-ΔC. Since it lacks the dimerization domain, eADF3-ΔC is monomeric in solution (MW = 95 kDa). Interestingly, liquid–liquid phase separation takes place even in the absence of the NR domain. eADF3-ΔC exhibits two phases at every tested pH value below pH 8.5; the protein concentrations and MWs are identical to those of solutions of eADF3 at pH 1 (see Figure 4b). This result indicates that the NR domain is not necessary for phase separation but can enforce it. We assume that the influence of the NR domain is based on the ionizable side chains of its glutamic and aspartic acid residues. At acidic pH the glutamic and aspartatic acids of the NR domain are likely protonated and, therefore, critically influence the net charge of the protein. Apparently this change leads to a decreased protein oligomerization potential and to a lower protein concentration in the high-density phase. Our experimental finding also explains why NR domains are critically involved in solubilizing spider silk proteins, as described previously.[6a]

Interestingly, the NR domain plays a crucial role in the lower critical solution temperature (LCST) behavior of the

recombinant spider silk protein. The low-density phase of eADF3, in contrast to that of eADF3-ΔC, displays fully reversible LCST behavior with a transition point at 25.4 °C (Figure 5), depending on protein concentration and ionic strength.

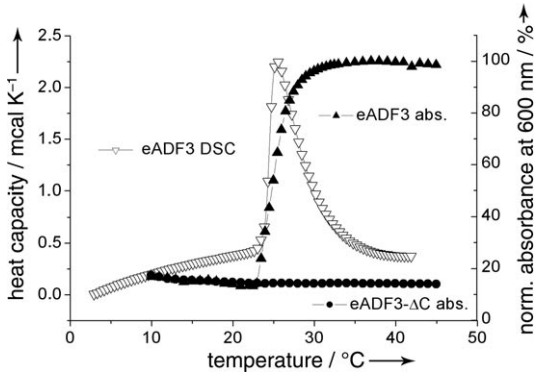

Figure 5. LCST behavior of the low-density phases of eADF3 and eADF3-ΔC at a concentration of 50 μM. LCST behavior was determined by turbidity measurements at 600 nm as well as by differential scanning calorimetry (DSC; only shown for eADF3). The LCST of eADF3 was determined to be 25.4 °C.

We conclude that liquid–liquid phase separation of the employed recombinant spider silk protein resembles an oligomerization process with physiological relevance for the spinning process. The high-density phase has properties similar to those found in the one-phase solution inside the spinning dope of the spider. In vitro phase separation is based on the amphiphilic nature of the large repetitive domains of the silk protein, while the NR domain enhances this effect. The NR domain is further crucial for LCST behavior. In summary, our finding provides the basis to establish an effective spinning process for recombinant spider silk proteins in vitro.

Experimental Section

Engineering of eADF3 and eADF3-ΔC: The amino acid sequence of eADF3 was adapted from the natural sequence of ADF3 from *Araneus diadematus*. Repetitive elements in the sequence of ADF3 display a polyalanine-rich motif, which was named A (sequence: GPYGPGASAAAAAAGGYGPGSGQQ), and a glutamine- and glycine-rich motif, which was named Q (sequence: GPGQQGPGQQGPGQQGPGQQ); the nonrepetitive carboxy terminus of ADF3 was referred to as NR (sequence: ASAAVSVGGYGPQSSSAPVASAAASRLSSPAASSRVSSAV-SSLVSSGPTNQAALSNTISSVVSQVSASNPGLSGCDVLVQALLEVVSA-LVSILGSSSIGQINYGASAQYTQMVGQSVAQALAG). Our previously established engineering approach allowed the combination and multimerization of the single motifs, resulting in two proteins: eADF3-ΔC, comprising 24 repeats each of modules A and Q, and eADF3, comprising $(AQ)_{24}$ and the NR domain.[6a]

Dialysis: Lyophilized proteins were dissolved in 6 M guanidinium thiocyanate (500 μM). Dialysis was performed against 10 mM tris(hydroxymethyl)aminomethane(Tris)/HCl, pH 8, at 4 °C using membranes with a molecular weight cut-off of 6000–8000 Da (Spectrum Laboratories, Rancho Dominguez, USA). The separated protein phases were stored at 4 °C. Control experiments were performed using additional buffer systems at the same pH:

pH	Buffer
1.0	HCl
5.0	10 mM citrate/HCl
7.0	10 mM 2-morpholinoethanesulfonic acid/NaOH
8.0	10 mM Tris/HCl
8.5	10 mM Tris/HCl (control: 10 mM ethanolamine/HCl)
9.0	10 mM ethanolamine/HCl (control: 10 mM glycine/NaOH)
10.0	10 mM $NaHCO_3/Na_2HCO_3$ (control: 10 mM glycine/NaOH)

Determination of protein concentrations: Protein concentrations were determined by UV measurements at 20 °C using a Cary100 spectrophotometer (Varian Medical Systems, Palo Alto, USA). For calculation of the protein concentration, the molar extinction coefficients of eADF3 ($75\,990\,M^{-1}cm^{-1}$) and eADF3-ΔC ($71\,520\,M^{-1}cm^{-1}$) at 280 nm and 20 °C were employed.

Circular dichroism (CD) measurements: Far-UV CD spectra were obtained using a Jasco 715 spectropolarimeter (Gross-Umstadt, Germany). All CD spectra were recorded using 1.5 μM protein solutions in 10 mM Tris/HCl, pH 8, in a 0.1-cm quartz cuvette at 20 °C. Control experiments employing the nondiluted phases in a 0.01-cm quartz cuvette led to identical results.

Lower critical solution temperature (LCST) analysis employing turbidity measurements: The solution turbidities of the low-density phase of eADF3 and eADF3-ΔC (50 μM each) were measured as a function of temperature. Optical densities at 600 nm were measured continuously using a Cary100 spectrophotometer while the samples were heated in 1-K increments. Maximum absorption of eADF3 was normalized to 100 %.

LCST analysis employing differential scanning calorimetry (DSC): DSC experiments were performed using a VP-DSC Micro-Calorimeter (MicroCal, Northampton, USA). Standard measurements were performed at a protein concentration of 50 μM in 10 mM Tris/HCl, pH 8, with a heating rate of $20\,K\,h^{-1}$.

Drawing of silk threads: A 10-μL portion of each phase of eADF3 was incubated up to 5 min in 0.5 M potassium phosphate, pH 8. Threads could be drawn with tweezers only out of the high-density protein phase.

Scanning electron microscopy (SEM): Silk threads were immobilized on Thermanox plastic cover slips (Nalge Nunc, USA), which had been coated with gold by sputtering under vacuum, and analyzed by a JSM 5900 LV scanning electron microscope (JEOL Ltd., Japan) at 20 kV.

Received: November 20, 2006
Revised: January 26, 2007
Published online: April 2, 2007

Keywords: calorimetry · phase transitions · protein engineering · self-assembly · silk spinning

[1] T. Scheibel, *Microb. Cell Fact.* **2004**, *3*, 14.
[2] J. M. Gosline, P. A. Guerette, C. S. Ortlepp, K. N. Savage, *J. Exp. Biol.* **1999**, *202*, 3295–3303.
[3] a) A. Lazaris, S. Arcidiacono, Y. Huang, J.-F. Zhou, F. Duguay, N. Chretien, E. A. Welsh, J. W. Soares, C. N. Karatzas, *Science* **2002**, *295*, 472–476; b) R. V. Lewis, *Acc. Chem. Res.* **1992**, *25*, 392–398; c) Y. Wang, H.-J. Kim, G. Vunkak-Novakovic, D. L. Kaplan, *Biomaterials* **2006**, *27*, 6064–6082; d) D. P. Knight, F. Vollrath, *Philos. Trans. R. Soc. London Ser. B* **2002**, *357*, 219–227; e) Z. Shao, F. Vollrath, *Nature* **2002**, *418*, 741.
[4] a) H.-J. Jin, D. L. Kaplan, *Nature* **2003**, *424*, 1057–1061; b) C. Zhou, B. Leng, J. Yao, J. Qian, X. Chen, P. Zhou, D. P. Knight, Z.

Shao, *Biomacromolecules* **2006**, *7*, 2145 – 2149; c) J. P. Zbilut, T. Scheibel, D. Huemmerich, C. L. Webber, M. Colafranceschi, A. Giuliani, *Phys. Lett. A* **2005**, *346*, 33 – 41; d) A. A. Dinerman, J. Cappello, H. Ghandehari, S. W. Hoag, *Biomaterials* **2002**, *23*, 4203 – 4210.

[5] a) A. Rising, H. Nimmervoll, S. Grip, A. Fernandez-Arias, E. Storckenfeldt, A. P. Knight, F. Vollrath, W. Engström, *Zool. Sci.* **2005**, *22*, 273 – 281; b) X. Chen, D. P. Knight, F. Vollrath, *Biomacromolecules* **2002**, *3*, 644 – 648.

[6] a) D. Huemmerich, C. W. Helsen, S. Quedzuweit, J. Oschmann, R. Rudolph, T. Scheibel, *Biochemistry* **2004**, *43*, 13604 – 13612; b) D. Huemmerich, U. Slotta, T. Scheibel, *Appl. Phys. A* **2005**, *82*, 219 – 222; c) U. Slotta, M. Tammer, F. Kremer, P. Koelsch, T. Scheibel, *Supramol. Chem.* **2006**, *18*, 465 – 471.

[7] C. Dicko, J. M. Kennedy, D. Knight, F. Vollrath, *Biochemistry* **2004**, *43*, 14080 – 14087.

